Memory effects in nonequilibrium quantum impurity models

Guy Cohen and Eran Rabani
School of Chemistry, The Sackler Faculty of Exact Sciences, Tel Aviv University, Tel Aviv 69978, Israel
(Received 26 May 2011; revised manuscript received 15 July 2011; published 12 August 2011)

Memory effects play a key role in the dynamics of strongly correlated systems driven out of equilibrium. In this paper, we explore the nature of memory in the nonequilibrium Anderson impurity model. The Nakajima-Zwanzig-Mori formalism is used to derive an exact generalized quantum master equation for the reduced density matrix of the interacting quantum dot, which includes a non-Markovian memory kernel. A real-time path integral formulation is developed in which all diagrams are stochastically sampled in order to numerically evaluate the memory kernel. We explore the effects of temperature down to the Kondo regime, as well as the role of source-drain-bias voltage and bandwidth on the memory. Typically, the memory decays on time scales significantly shorter than the dynamics of the reduced density matrix itself, yet under certain conditions, it develops a low magnitude but long-ranged tail. In addition, we address the conditions required for the existence, uniqueness, and stability of a steady state.

DOI: 10.1103/PhysRevB.84.075150 PACS number(s): 71.10.Fd, 05.10.−a, 05.30.−d

I. INTRODUCTION

Interest in the problem of intrinsically *nonequilibrium* open quantum systems, in which one considers a small, strongly interacting, and highly correlated region coupled to several large, noninteracting baths, has been surging in both experiment and theory. The aim of theory in this regard is to provide a solid framework for understanding phenomena ranging from the nonequilibrium Kondo effect in quantum dots to conductance through single molecules.[1] While much progress has been made recently, based on brute-force approaches such as time-dependent numerical renormalization-group techniques[2–4] and iterative[5,6] or stochastic[7–9] diagrammatic approaches to real-time path integral formulations, the problem has never been fully solved in a satisfactory manner. In fact, it is becoming clearer that major gaps exist in our understanding of the dynamics, the crossover regimes, the dependence on initial conditions, and the behavior at steady state.

The kind of open systems discussed above are often addressed by impurity models, which explicitly account for the two types of regions within the problem by partitioning the Hamiltonian into system and bath subspaces: $H = H_S + H_B + V$, where H_S represents a low-dimensional but interacting "system" subspace, H_B represents a set of noninteracting lead or bath subspaces, and V is a system-bath coupling term. The dynamics generated by such Hamiltonians can feature transients on time scales that are much longer than the typical inverse energy scale,[10] where numerically exact approaches become intractable due to the exponential growth of the active space or the equivalent complications resulting from the dynamical sign problem. In many important situations, however, the noninteracting baths can be traced out, leading to a reduced description of the dynamics of the interacting system at the cost of introducing nonlocality in the time propagation.[11] In path integral approaches, the effects of the leads are accounted for by a time nonlocal influence functional.[5,7]

Perhaps a more appealing approach, which has been used to derive very successful perturbative schemes for fermionic systems[12–14] but is notoriously difficult to carry out exactly, is based on the generalized quantum master equation (GQME). In this formalism, a so-called memory kernel replaces the influence functional. The complexity of solving the many-body quantum Liouville equation is then reduced to the evaluation of this memory kernel, which fully determines the dynamics of the system. Furthermore, the memory kernel contains all the information needed to resolve questions concerning the existence and uniqueness of a steady state,[15,16] as well as the values of system observables at steady state. While the dynamical time scale of the system typically exceeds the characteristic inverse energy scale, the memory kernel is expected to decay on relatively short time scales for a large and interesting class of physical situations (essentially whenever the bandwidth of the baths is much larger than other energy scales in the problem). Thus, brute-force approaches limited to short times are well suited to its calculation. Once the memory function is known, the formalism is exact and tractable at *all* times.

In this paper, we explore the nature of memory in nonequilibrium impurity models, focusing on the Anderson problem.[17] We cover the effects of temperature down to the Kondo regime, as well as the role of source-drain-bias voltages and bandwidth. This is accomplished by adopting the Nakajima-Zwanzig-Mori[18–20] formalism to derive a *formally exact* GQME for the reduced density matrix $\sigma(t) = P\rho(t)$ of the interacting system, which includes a non-Markovian memory kernel. The kernel of this equation is then evaluated in a *numerically exact* fashion by way of the real-time path integral Monte Carlo (RT-PIMC) method. The conjecture that the memory decays on time scales significantly shorter than the dynamics of $\sigma(t)$ is confirmed, yet it is found that it develops a smaller long tail when the Hubbard term is switched on. The approach provides means to simulate the dynamics of the strongly correlated subsystem on time scales beyond the limits of the path integral method itself and reveals the conditions required for the existence, uniqueness, and stability of a steady state under a finite source-drain bias.

The outline is as follows: In Sec. II, we discuss the formulation of the GQME and its application to the nonequilibrium Anderson model in a form amenable to path integral treatment. This is accompanied in Sec. III by a brief explanation of the

 ©2011 American Physical Society

real-time path integral Monte Carlo method as applied to the memory kernel. Then, in Sec. IV, we display and analyze the results of some explicit calculations we have carried out. Finally, in Sec. V, we conclude.

II. GENERALIZED QUANTUM MASTER EQUATION

The exact equation of motion of the complete density matrix $i\hbar\frac{d}{dt}\rho = [H,\rho]$ is governed by the Liouvillian $\mathcal{L} = [H,\ldots]$. If the coupling term V were to be turned off, the dynamics of the two subspaces would be given by similar equations with the Liouvillian replaced by the system and bath Liouvillians, defined, respectively, as

$$\mathcal{L}_S = [H_S,\ldots], \tag{1}$$

$$\mathcal{L}_B = [H_B,\ldots]. \tag{2}$$

We also define a coupling Liouvillian

$$\mathcal{L}_V = [V,\ldots]. \tag{3}$$

The equation of motion for the reduced density operator

$$\rho_B\sigma = P\rho, \tag{4}$$

$$P \equiv \rho_B \mathrm{Tr}_B\{\ldots\} \tag{5}$$

(using the projection operator P onto the system subspace) is then given by

$$i\hbar\frac{d}{dt}\sigma(t) = \mathcal{L}_S\sigma(t) + \vartheta(t) - \frac{i}{\hbar}\int_0^t d\tau\,\kappa(\tau)\sigma(t-\tau), \tag{6}$$

where

$$\vartheta(t) = \mathrm{Tr}_B\left\{\mathcal{L}_V e^{-\frac{i}{\hbar}Q\mathcal{L}t}Q\rho_0\right\} \tag{7}$$

contains the initial correlations

$$\kappa(t) = \mathrm{Tr}_B\{\mathcal{L}_V e^{-iQ\mathcal{L}\tau}Q\mathcal{L}\rho_B\} \tag{8}$$

is the memory kernel in superoperator form, and

$$Q = 1 - P \tag{9}$$

is the projection operator onto the complementary subspace. The initial conditions are contained within the initial density matrix ρ_0, which also determines the initial bath part of the density matrix $\rho_B = Q\rho_0$.

The above equation for $\sigma(t)$ is exact, yet requires as input the two superoperator functions $\kappa(t)$ and $\vartheta(t)$, both of which have been defined in terms of projected propagation. Evaluating such projected dynamics is cumbersome and can be reduced to solving a superoperator Volterra equation of the second type involving a quantity $\Phi(t)$, which is free of projected propagation.[21,22] For the memory kernel, one finds

$$\kappa(\tau) = i\hbar\dot{\Phi}(\tau) - \Phi(\tau)\mathcal{L}_S + \frac{i}{\hbar}\int_0^\tau d\tau\,\Phi(t-\tau)\kappa(\tau), \tag{10}$$

$$\Phi(t) = \mathrm{Tr}_B\left\{\mathcal{L}_V e^{-\frac{i}{\hbar}\mathcal{L}t}\rho_B\right\}. \tag{11}$$

A similar procedure exists for the initial correlation term ϑ; however, here we consider only the initially factorized case $\rho_0 = \rho_B\otimes\sigma(0)$, for which $\vartheta = 0$. As discussed below, the matrix elements of the superoperator Φ are almost identical to quantities to which RT-PIMC has already been applied.[7,8]

In the Anderson impurity model,

$$H_S = \sum_{i=\uparrow\downarrow}\varepsilon_i d_i^\dagger d_i + U d_\uparrow^\dagger d_\uparrow d_\downarrow^\dagger d_\downarrow, \tag{12}$$

$$H_B = \sum_{k,i=\uparrow\downarrow}\varepsilon_{ik}a_{ik}^\dagger a_{ik}, \tag{13}$$

$$V = \sum_{k,i=\uparrow\downarrow} t_{ik}d_i a_{ik}^\dagger + t_{ik}^* a_{ik}d_i^\dagger. \tag{14}$$

Thus, the system subspace is four dimensional, being spanned by the states $0\equiv|00\rangle\equiv|0\rangle$, $1\equiv|01\rangle = d_\downarrow^\dagger|0\rangle$, $2\equiv|10\rangle = d_\uparrow^\dagger|0\rangle$, and $3\equiv|11\rangle = d_\uparrow^\dagger d_\downarrow^\dagger|0\rangle$. With this notation, we can perform a calculation to derive an expression for the system Liouvillian

$$\begin{aligned}[\mathcal{L}_s]_{ij,qq'} = \delta_{iq}\delta_{jq'}\{&\varepsilon_\uparrow(\delta_{q2}+\delta_{q3}-\delta_{j2}-\delta_{j3})\\ &+\varepsilon_\downarrow(\delta_{q1}+\delta_{q3}-\delta_{j1}-\delta_{j3})\\ &+U(\delta_{q3}-\delta_{j3})\},\end{aligned} \tag{15}$$

and for Φ, which takes the more complicated form

$$\begin{aligned}\Phi_{ij,qq'} = &-\delta_{i2}\delta_{j1}\left(\psi_{qq'}^{(1)} - \psi_{qq'}^{(2)*}\right) - \delta_{i1}\delta_{j2}\left(\psi_{qq'}^{(2)} - \psi_{qq'}^{(1)*}\right)\\ &+\delta_{ij0}\left(\varphi_{qq'}^{(1)} + \varphi_{qq'}^{(3)}\right) + \delta_{ij1}\left(\varphi_{qq'}^{(2)} - \varphi_{qq'}^{(3)}\right)\\ &+\delta_{ij2}\left(-\varphi_{qq'}^{(1)} + \varphi_{qq'}^{(4)}\right) + \delta_{ij3}\left(-\varphi_{qq'}^{(2)} - \varphi_{qq'}^{(4)}\right),\end{aligned} \tag{16}$$

$$\varphi_{qq'}^{(m)} = 2i\Im\sum_k \mathrm{Tr}_B\left\{\rho_B\langle q'|A_k^{(m)}|q\rangle\right\}, \tag{17}$$

$$\psi_{qq'}^{(m)} = -2\sum_k \mathrm{Tr}_B\left\{\rho_B\langle q'|B_k^{(m)}|q\rangle\right\}, \tag{18}$$

where $A_k^{(1)} = t_{\uparrow k}d_\uparrow d_\downarrow d_\downarrow^\dagger a_{\uparrow k}^\dagger$, $A_k^{(2)} = t_{\uparrow k}d_\uparrow d_\downarrow^\dagger d_\downarrow a_{\uparrow k}^\dagger$, $A_k^{(3)} = t_{\downarrow k}d_\uparrow d_\uparrow^\dagger d_\downarrow a_{\downarrow k}^\dagger$, $A_k^{(4)} = t_{\downarrow k}d_\uparrow^\dagger d_\uparrow d_\downarrow a_{\downarrow k}^\dagger$, $B_k^{(1)} = t_{\uparrow k}d_\downarrow a_{\uparrow k}^\dagger$, and $B_k^{(2)} = t_{\downarrow k}d_\uparrow a_{\downarrow k}^\dagger$. All the quantities in (16)–(18) are implicitly time dependent and can be evaluated directly with RT-PIMC (as outlined in Sec. III).

One can draw a few analytical conclusions directly from the block structure of Φ. First, while both the $A_k^{(m)}$ and $B_k^{(m)}$ operators introduced above conserve the total particle number, only the $A_k^{(m)}$ conserve the particle number for *each* spin. Therefore, the $\psi_{qq'}^{(m)}$ are nonzero only if $q,q' = 1,2$ or $2,1$ (since states 1 and 2 are the only dot states that have the same total occupation, but differ in per-spin occupation), while the $\varphi_{qq'}^{(m)}$ can be nonzero only when $q = q'$. From (16), we can then immediately see that the diagonal density matrix elements are coupled only to each other, with the two singly occupied off-diagonal elements $|1\rangle\langle 2|$ and $|2\rangle\langle 1|$ forming a second closed block. If our interest is limited to the state populations, only the 16 (instead of 64) functions $\varphi_{qq}^{(m)}$ need be evaluated within RT-PIMC.

III. PATH INTEGRAL MONTE CARLO

To apply the RT-PIMC method[7,8,23] to the quantities above, we express them in terms of a summation of influence functionals over all possible dot occupations at every point in time. The set of occupations as a function of time, referred to as the "paths," forms the Monte Carlo configuration space,

which scales exponentially in size with the number of dot electrons and the time. In essence, one estimates the sum over all paths by performing a partial weighted sum: consider an observable A having the influence functional A_σ, where σ denotes a path. If w_σ is some so-called weight functional, then

$$\langle A\rangle = \sum_\sigma A_\sigma = \sum_\sigma \frac{A_\sigma}{w_\sigma}\omega_\sigma = \left\langle \frac{A}{w}\right\rangle_w . \tag{19}$$

The weighted sum of this last expression can be evaluated to numerical exactness by using the standard Metropolis algorithm, with the rate of convergence largely determined by the weight.

To work out the influence functional relating to observables of the form $\varphi_{qq'}(t) = \mathrm{Tr}_B\{\rho_B\langle q'|A(t)|q\rangle\} = \mathrm{Tr}\{|q\rangle\langle q'|\rho_B A(t)\}$, as in (17) and (18), one rewrites it in the interaction picture (with $H_0 = H_S + H_B$) as follows:

$$\varphi_{qq'}(t) = \mathrm{Tr}\big\{|q\rangle\langle q'|\rho_B U_I^\dagger(t)A_{H_0}(t)U_I(t)\big\}. \tag{20}$$

Note that if we define $\rho_0 = |q\rangle\langle q'|\rho_B$, the system indices q and q' can be interpreted as defining the dot part of the initial density matrix, and that the initial conditions remain uncorrelated with this definition. With this in mind, we continue by expanding the unitary propagator $U_I^\dagger$ and its adjoint in the time-ordered Dyson series

$$U_I^\dagger(t) = \sum_{n=0}^{\infty}\left(\frac{i}{\hbar}\right)^n \int_0^t ds_1 \int_0^{s_1} ds_2 \ldots \int_0^{s_{n-1}} ds_n \times V_{H_0}(s_1)V_{H_0}(s_2),\ldots,V_{H_0}(s_n). \tag{21}$$

Since applying the operator V always modifies the dot occupations, this leads to an expression that can easily be interpreted as a path integral over the σ space:

$$\begin{aligned}\varphi_{qq'}(t) = \sum_{n,n'=0}^{\infty}(-1)^{n'}\left(\frac{i}{\hbar}\right)^{n+n'} \mathrm{Tr}\Big\{&|q\rangle\langle q'|\rho_B \\ &\times \int_0^t ds_1 \int_0^{s_1} ds_2 \ldots \int_0^{s_{n-1}} ds_n \\ &\times \int_0^t ds'_1 \int_0^{s'_1} ds'_2 \ldots \int_0^{s'_{n'-1}} ds'_{n'} \\ &\times V_{H_0}(s_1)V_{H_0}(s_2),\ldots,V_{H_0}(s_n)A_I(t) \\ &\times V_{H_0}(s'_1)V_{H_0}(s'_2),\ldots,V_{H_0}(s'_{n'})\Big\}\end{aligned} \tag{22}$$

$$\equiv \int \mathcal{D}\left(\sigma,\sigma'\right)\mathcal{F}_{qq'}\left(\sigma,\sigma'\right). \tag{23}$$

From (14), we can see that $V = V^\uparrow + V^\downarrow$ is the sum of terms involving different spins. The paths σ and σ' therefore uniquely determine n and n', the times $\{s_i\}$ and $\{s'_i\}$, and the spins $\{\chi_i\}$ and $\{\chi'_i\}$ associated with each such time.

Since it is possible to obtain exact analytical expressions for the interaction picture operators $A_{H_0}(t)$ and $V_{H_0}(t)$ in all cases of interest here, $\mathcal{F}(\sigma,\sigma')$ is always a product of simple functions of time and traces over operator products at time zero (when the system is at thermal equilibrium and Wick's rule can be applied). Specifically, if we write

$$\varphi^{(m)}_{qq'} = 2i\Im\int \mathcal{D}(\sigma,\sigma')\mathcal{F}^{(m)}_{qq'}(\sigma,\sigma'), \tag{24}$$

then, from comparing with (23),

$$\begin{aligned}\mathcal{F}^{(i)}_{qq'}(\sigma,\sigma') = (-1)^{n'}\left(\frac{i}{\hbar}\right)^{n+n'}\mathrm{Tr}\Big\{&|q\rangle\langle q'|\rho_B \\ &\times V^{\chi_1}_{H_0}(s_1)V^{\chi_2}_{H_0}(s_2),\ldots,V^{\chi_n}_{H_0}(s_n)\sum_k A^{(i)}_k \\ &\times V^{\chi'_1}_{H_0}(s'_1)V^{\chi'_2}_{H_0}(s'_2),\ldots,V^{\chi'_{n'}}_{H_0}(s'_{n'})\Big\}.\end{aligned} \tag{25}$$

The evaluation of traces of this kind within the Anderson model has been addressed in the literature before.[8]

IV. RESULTS

In Fig. 1, we plot the nonzero elements of the memory kernel for different values of U. Due to the block structure and the symmetric choice of parameters, only seven distinct nonzero elements exist (two for $U = 0$). To make the parametrization definite within the simulations, we assume lead coupling densities of the form $\Gamma_i(E) \equiv 2\pi\sum_k |t_k|^2\delta(E - \varepsilon_{ik}) = \frac{\Gamma/2}{(1+e^{\nu(E-\varepsilon_c)})(1+e^{-\nu(E+\varepsilon_c)})}$, where ε_c is the band cutoff energy and ν is the inverse of the cutoff width. Γ is the maximum value attainable by $\Gamma(E) = \sum_i \Gamma_i(E)$, as well as its wide-band limit, and will be the unit of energy throughout the following text. We also concentrate on $\varepsilon_i = -\frac{U}{2}$, known as the symmetric case of the Anderson model, yet the formalism is general and this is certainly not a requirement. The temperature β and the chemical potentials μ_L and μ_R enter the calculation

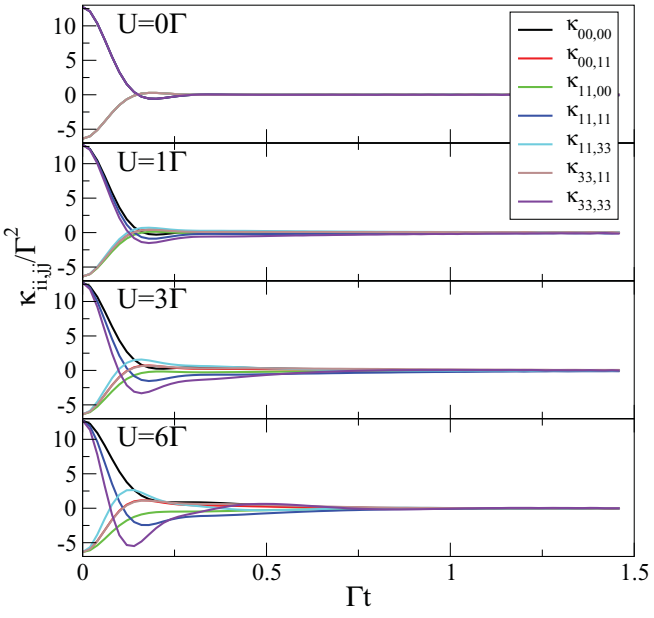

FIG. 1. (Color online) Distinct nonzero memory-kernel elements for an initially unoccupied dot and several values of the interaction energy U. The remaining parameters are $\frac{\mu_L}{\Gamma} = -\frac{\mu_R}{\Gamma} = \frac{1}{2}$, $\frac{\varepsilon_c}{\Gamma} = 20$, and $\beta\Gamma = 1$.

through ρ_B at time zero, for which we assume the proper grand canonical distribution.

In the noninteracting case (top panel of Fig. 1), a rapid decay to zero is observed. Despite the relatively broad and soft-edged band chosen here, the decay occurs over a time scale smaller than the inverse coupling but comparable to it. We can learn from this that any approximation based on short memory should be expected to fail unless it can allow for memories of at least this length, meaning, for instance, that Markovian approaches to the problem can not be expected to succeed in general (consider how Redfield master equations fail to capture the level broadening, which is so easy to obtain within the simple Landauer formalism). As U is increased, it becomes clear that the interaction, despite breaking most of the symmetries between the various elements, does not significantly affect memory decay on the first time scale. However, even at very small interaction energies, a second, longer time scale develops: at this time scale, a small part of each memory-kernel element decays more slowly.

The formalism becomes extremely interesting if having the memory as an input only up to some finite cutoff time t_c (at which the system's dynamics have not yet died out) allows accurate predictions at far longer times. This will occur if the memory function has essentially gone to zero by this time, such that it can be safely truncated. In the left panels of Fig. 2, we plot the time derivative of the total population (dP/dt) and show that, for certain noninteracting parameters, this does indeed happen: once $\Gamma t_c \gtrsim 0.3$ dynamics at times over an order of magnitude greater than those of the memory kernel are reliably reproduced, and the exact steady-state result for all diagonal elements of σ is obtained to within the numerical errors and shown on the top right panel of Fig. 2. However, as might be expected from the analysis of Fig. 1, in the strongly correlated cases, a short cutoff time results in incorrect populations when propagated for much longer times than t_c since truncating the memory at that point has not yet become physically reasonable. For the cases of $U = \Gamma$ and $U = 6\Gamma$,

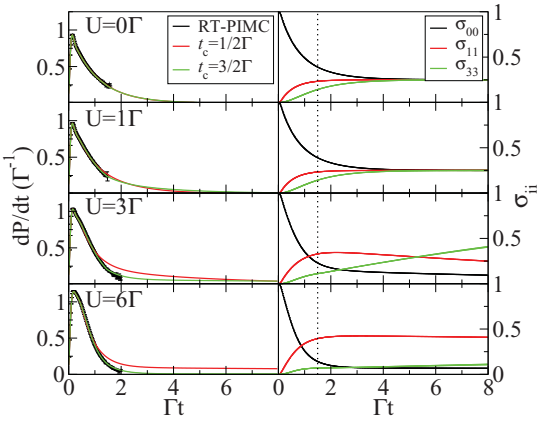

FIG. 2. (Color online) Total population derivative from direct RT-PIMC data compared with the results of the memory-kernel formalism (left panels) and predicted dot populations (right panels) for an initially unoccupied dot for several values of the interaction energy U. Remaining parameters are the same as in Fig. 1. The cutoff time is $\frac{1.5}{\Gamma}$, shown on the right panels as a vertical dotted line.

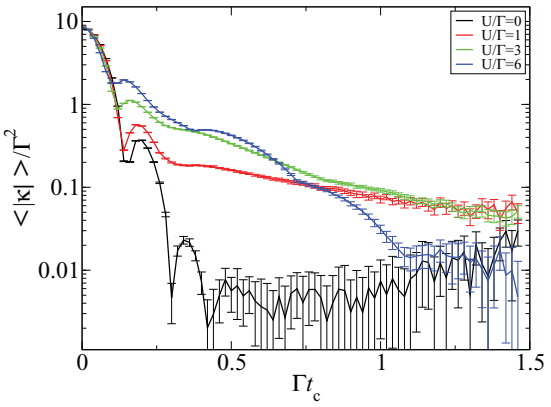

FIG. 3. (Color online) The average absolute value of memory-kernel elements at $\frac{\mu_L}{\Gamma} = -\frac{\mu_R}{\Gamma} = \frac{1}{2}$, $\frac{\varepsilon_c}{\Gamma} = 20$, $\beta\Gamma = 1$, and different values of the interaction energy U.

the qualitative physics is captured correctly within $\Gamma t_c = 1.5$ in that depopulation of the zero-electron level is accelerated at short times; for $U = 6\Gamma$, one also observes that at longer times the one-electron levels draw most of the population, while the more energetic zero- and two-electron levels are suppressed. However, for $U = 3\Gamma$, the behavior predicted by the truncated memory function is clearly wrong, suggesting that the long tails are of greater importance in this case.

Figures 3 and 4 explore the decay of the memory-kernel elements more clearly by plotting the average absolute value of the memory-kernel elements on a logarithmic scale, for various values of U, ε_c, and β. Notably, while only the noninteracting case appears to have a memory kernel that goes to within the numerical errors of zero during the simulation time scale shown here, strong interaction actually appears to reduce the memory lifetime when compared with intermediate values. This relates to the fact the $U = 3\Gamma$ problem is "harder" in this sense than the strongly interacting $U = 6\Gamma$ problem, as discussed above. While increasing either the bandwidth or the temperature appears to affect the short-term behavior, by reducing the shorter memory time scale, the longer time scale appears largely unaffected by the variation of these parameters. This observation seems to be consistent with the hypothesis that the time scale of the tail's memory decay is related to the

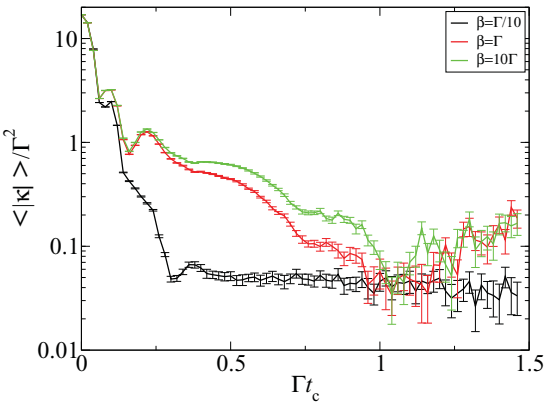

FIG. 4. (Color online) The average absolute value of memory-kernel elements at $\mu_L = \mu_R = 0$, $\frac{\varepsilon_c}{\Gamma} = 40$, $\frac{U}{\Gamma} = 6$, and different temperatures β.

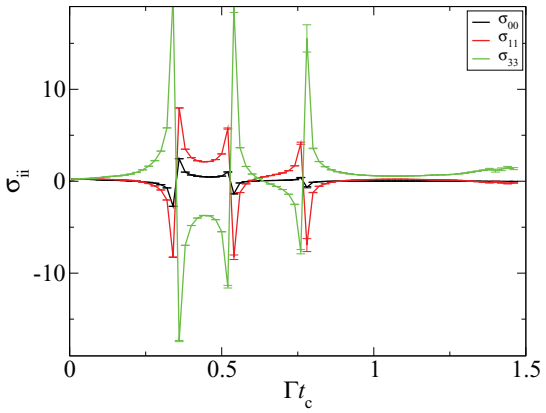

FIG. 5. (Color online) The predicted steady-state values of the diagonal density matrix elements at $\frac{\mu_L}{\Gamma} = -\frac{\mu_R}{\Gamma} = \frac{1}{2}$, $\frac{\varepsilon_c}{\Gamma} = 20$, $\beta\Gamma = 1$, and $\frac{U}{\Gamma} = 6$.

inverse Kondo temperature. However, we find that a large bias voltage does not affect markedly the longer time scale, despite supposedly destroying the Kondo correlations.

In addition to the time dependence, one can obtain the steady-state result directly from the stationary state equation

$$\left[\mathcal{L}_S - \frac{i}{\hbar}\hat{\kappa}(z \to i0)\right]\sigma(t \to \infty) = \lim_{z\to 0} z\hat{v}(z) \qquad (26)$$

with the added condition that $\mathrm{Tr}\sigma = 1$. This means that, for an initially uncorrelated system, a unique steady state exists if and only if the supermatrix $\mathrm{Tr}_S\{(|i\rangle\langle j|)^\dagger[\mathcal{L}_S - \frac{i}{\hbar}\hat{\kappa}(z \to i0)]|k\rangle\langle l|\}$ has a degeneracy of exactly one. In Fig. 5, the steady-state values obtained from this formula for parameters close to the Kondo regime are plotted against the cutoff time t_c. While the trace of the density matrix is conserved, physically impossible results appear at intermediate cutoff times and convergence is not yet achieved. The long tails of the memory-kernel elements are therefore crucially important for the correct prediction of both dynamical and steady-state properties. In this context, this fact is significant not only physically, but also computationally, since the complexity scales exponentially with the simulation time.

V. SUMMARY AND CONCLUSIONS

In conclusion, we have developed a numerically exact method for the formulation and solution of the reduced dynamics of quantum impurity models and applied it to the nonequilibrium Anderson model. It is clear from our results that the physics of even a noninteracting electronic junction can not be fully captured within a Markovian picture, and that on-site interaction results in deeply non-Markovian physics even at relatively large bandwidths, bias voltages, and temperatures. We show that the long memory tails induced by the Hubbard term affect both the dynamics and the steady state, despite their relative smallness.

In the computational sense, the proposed method is extremely useful in extending the applicability of RT-PIMC to long time scales and steady state when the memory goes to zero within the simulation time scale, but the dynamics do not. Improvement of the PIMC scheme is required in situations where the memory kernel does not decay within the simulations time scale (see the case for $U = 3\Gamma$). One possible route is based on combining the present formalism with the new sampling technique based on the noncrossing approximation.[24] This and other scenarios for improving the PIMC scheme are currently under study.

ACKNOWLEDGMENTS

The authors would like to thank A. Nitzan and D. Reichman for useful discussion. G.C. is grateful to the Azrieli Foundation for the award of an Azrieli Fellowship. E.R. thanks the Miller Institute for Basic Research in Science at UC Berkeley for partial financial support via a Visiting Miller Professorship. This work was supported by the US-Israel Binational Science Foundation and by the FP7 Marie Curie IOF project HJSC.

[1] A. Nitzan and M. A. Ratner, Science **300**, 1384 (2003).
[2] F. B. Anders and A. Schiller, Phys. Rev. Lett. **95**, 196801 (2005).
[3] S. R. White, Phys. Rev. Lett. **69**, 2863 (1992).
[4] P. Schmitteckert, Phys. Rev. B **70**, 121302 (2004).
[5] S. Weiss, J. Eckel, M. Thorwart, and R. Egger, Phys. Rev. B **77**, 195316 (2008).
[6] D. Segal, A. J. Millis, and D. R. Reichman, Phys. Rev. B **82**, 205323 (2010).
[7] L. Mühlbacher and E. Rabani, Phys. Rev. Lett. **100**, 176403 (2008).
[8] P. Werner, T. Oka, and A. J. Millis, Phys. Rev. B **79**, 035320 (2009).
[9] M. Schiró and M. Fabrizio, Phys. Rev. B **79**, 153302 (2009).
[10] P. Nordlander, M. Pustilnik, Y. Meir, N. S. Wingreen, and D. C. Langreth, Phys. Rev. Lett. **83**, 808 (1999).
[11] R. P. Feynman and F. L. Vernon, Ann. Phys. (NY) **24**, 118 (1963).
[12] M. Leijnse and M. R. Wegewijs, Phys. Rev. B **78**, 235424 (2008).
[13] H. Schoeller, Eur. Phys. J. Special Topics **168**, 88 (2009).
[14] G. Q. Li, B. D. Fainberg, A. Nitzan, S. Kohler, and P. Hänggi, Phys. Rev. B **81**, 165310 (2010).
[15] A. Dhar and D. Sen, Phys. Rev. B **73**, 085119 (2006).
[16] E. Khosravi, G. Stefanucci, S. Kurth, and E. K. U. Gross, PhysChemChemPhys **11**, 4535 (2009).
[17] P. W. Anderson, Phys. Rev. **124**, 41 (1961).
[18] S. Nakajima, Prog. Theor. Phys. **20**, 948 (1958).
[19] R. Zwanzig, J. Chem. Phys. **33**, 1338 (1960).
[20] H. Mori, Prog. Theor. Phys. **33**, 423 (1965).
[21] R. Zwanzig, *Nonequilibrium Statistical Mechanics* (Oxford University Press, New York, 2001).
[22] M. Zhang, B. J. Ka, and E. Geva, J. Chem. Phys. **125**, 044106 (2006).
[23] L. Muehlbacher, D. F. Urban, and A. Komnik, Phys. Rev. B **83**, 075107 (2011).
[24] E. Gull, D. R. Reichman, and A. J. Millis, e-print arXiv:1105.1175.